PROCEEDINGS OF SCIENCE

B_s decay and charmed hadronic B decay

Jin Li[*†]
University of Hawaii
E-mail: lijin@phys.hawaii.edu

We report on recent results from B_s and charmed B decay. The topics include $\Upsilon(5S)$ decays to B mesons, $B_s \to D_s^-(K/\pi), J/\psi\eta$, B_s semileptonic decay, B meson baryonic decay, doubly charmed decay through $b \to c\bar{c}s$ and singly charmed decay through $(b \to c\bar{u}d + s\bar{s}$ popping$)$.

Flavor Physics & CP Violation 2009
May 27 - June 1, 2009
Lake Placid, NY, USA

*Speaker.
†The FPCP09 organizer

PoS(FPCP2009)038

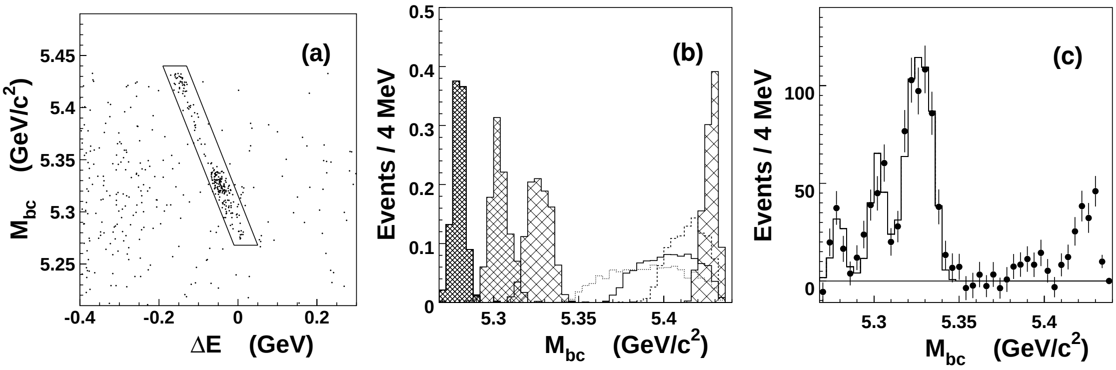

Figure 1: (a) The $M_{\rm bc}, \Delta E$ scatter plot for $B^+ \to J/\psi K^+$. The superimposed parallelogram indicates the $(M_{\rm bc} + \Delta E - 5.28)$ signal region. (b) Simulated $M_{\rm bc}$ distributions for $B^0 \to D^-\pi^+$ in MC. The channels $B\bar{B}$, $B\bar{B}^* + B^*\bar{B}$, $B^*\bar{B}^*$ and $B\bar{B}\pi\pi$ are shown as hatched histograms in the order of increasing hatching cell size from left to right, while the $B\bar{B}\pi$, $B\bar{B}^*\pi + B^*\bar{B}\pi$, $B^*\bar{B}^*\pi$ are represented in dotted, normal, and dashed histograms. (c) Background subtracted $M_{\rm bc}$ distribution for data, along with the fit histograms for 2 body channels (solid line).

1. $\Upsilon(5S)$ and B_s decay

The KEKB accelerator in Japan has been running very smoothly on the $\Upsilon(5S)$ resonance, leading to a large number of B_s mesons that were detected in the Belle detector. By the end of 2009, there will be $\sim 100 \text{fb}^{-1}$ $\Upsilon(5S)$ data collected at Belle. In this paper, we report on results from 23.6 fb^{-1} data collected on the $\Upsilon(5S)$ resonance using the Belle detector from 2005 and 2006, where 1.39M $B_s^{(*)}B_s^{(*)}$ pairs were produced.

The total $b\bar{b}$ cross section at the $\Upsilon(5S)$ energy has been measured to be (0.302 ± 0.014) nb, in which the fraction to $B_s^{(*)}B_s^{(*)}$ pair has been measured to be $f_s = N_{B_s^{(*)}B_s^{(*)}}/N_{b\bar{b}} = (19.5^{+3.0}_{-2.3})\%$ [1, 2]. In the study of B_s decays, we generally calculate two variables: the beam-constrained mass $M_{\rm bc} = \sqrt{E_b^{*2} - \vec{p}_{B_s}^{*2}}$ and the energy difference $\Delta E = E_{B_s}^* - E_b^*$, where $(E_{B_s}^*, \vec{p}_{B_s}^*)$ is the four-momentum of the reconstructed B_s candidate in the $\Upsilon(5S)$ CM frame.

Belle has studied the 3/4 body decay of $\Upsilon(5S) \to B^{(*)}B^{(*)}\pi(\pi)$, where B means B_u or B_d. Only one B meson is reconstructed in 5 submodes $(B^+ \to J/\psi K^+, \bar{D}^0(K^-\pi^+)\pi^+, \bar{D}^0(K^-3\pi)\pi^+; B^0 \to J/\psi K^{*0}, D^-(K^+\pi^-\pi^-)\pi^+)$. Fig. 1(a) shows the scatter plot of the $B \to J/\psi K^+$ channel in data. By fitting the distributions of the value $M_{\rm bc} + \Delta E - 5.28$ in bins of $M_{\rm bc}$, the B meson signal yields are extracted as a function M_{bc}(Fig. 1(c)). The MC distributions in Fig. 1(b) shows that the 2/3/4 body decay channel of $\Upsilon(5S)$ can be distinguished in $M_{\rm bc}$, which is due to different B momentum in $\Upsilon(5S)$ rest frame in different channels. An enhancement in high $M_{\rm bc}$ region in background subtracted data (Fig. 1(c)) corresponding to $\Upsilon(5S)$'s 3 or 4 body decays is seen, along with the peaks in low $M_{\rm bc}$ region. The branching fractions for 2 body decays $\Upsilon(5S) \to B^{(*)}B^{(*)}$ are extracted by performing a fit in the region $5.268 < M_{\rm bc} < 5.348$ GeV to Fig. 1(c). The branching fraction for 3/4 body decay is obtained by fitting $M_{\rm bc} + \Delta E - 5.28$ in the region $5.348 < M_{\rm bc} < 5.44$ GeV, as $\mathscr{B}(\Upsilon(5S) \to B^{(*)}B^{(*)}\pi(\pi)) = (17.0^{+1.6}_{-1.5} \pm 2.7)\%$, which is inconsistent with theoretical calculations $(\sim 0.03\%)$ [3].

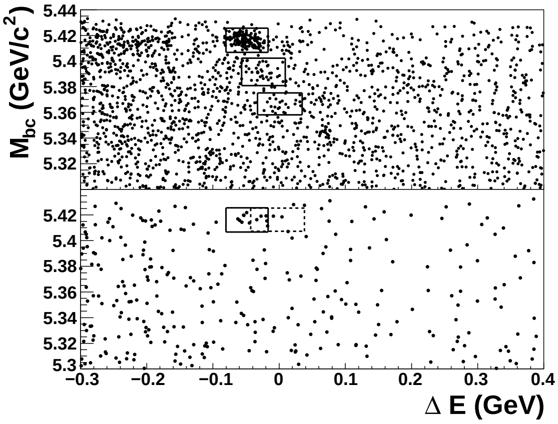

Figure 2: Scatter plots for $B_s \to D_s^- \pi^+$ (top) and $B_s \to D_s^{\mp} K^{\pm}$ (bottom). The three boxes in the top plot are the signal regions for $\Upsilon(5S) \to B_s^* \bar{B}_s^*, B_s^* \bar{B}_s^0, B_s^0 \bar{B}_s^0$, from top to bottom. The dashed box is the region where background from $B_s \to D_s^- \pi^+$ sits.

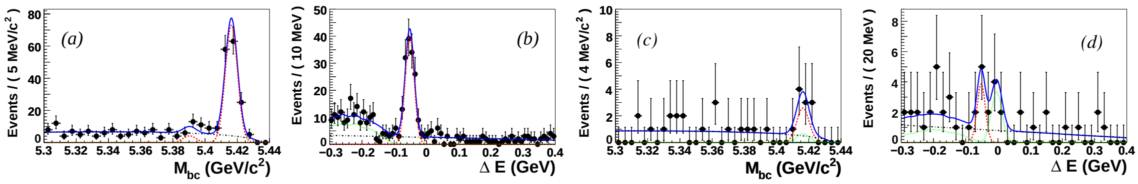

Figure 3: (a,c) $M_{\rm bc}$ distributions for candidates in the $B_s^* B_s^*$ ΔE signal region, (b,d) ΔE distributions for events in the $B_s^* B_s^*$ $M_{\rm bc}$ signal region, for $B_s \to D_s^- \pi^+$ (a,b) and $B_s \to D_s^{\mp} K^{\pm}$ (c,d) modes. The dotted curves in (b) and (d) represent the $B_s \to D_s^{*-} \pi^+$ and $B_s \to D_s^{(*)-} \pi^+$ background.

1.1 Measurement of the decays $B_s \to D_s^- \pi^+$ and $B_s \to D_s^{\mp} K^{\pm}$

The decay $B_s \to D_s^- \pi^+$ proceeds through a Cabibbo-favored tree process, and has a large branching fraction which may serve as a normalization mode for B_s decays. The decay $B_s \to D_s^- K^+$ is Cabibbo-suppressed and is an important decay channel in measuring the weak phase gamma through time-dependent CP violation measurements.

Belle measured the branching fractions of $B_s \to D_s^- \pi^+ (K^+)$, by fitting the 2D distributions of ΔE and $M_{\rm bc}$. Fig. 2 shows the scatter plots for $B_s^0 \to D_s^- \pi^+$ and $B_s^0 \to D_s^{\mp} K^{\pm}$. The fit curves are shown in Fig. 3. We obtain [4] $\mathscr{B}(B_s^0 \to D_s^- \pi^+) = [3.67^{+0.35}_{-0.33}(\text{stat.})^{+0.43}_{-0.42}(\text{syst.}) \pm 0.49(f_s)] \times 10^{-3}$, and $\mathscr{B}(B_s^0 \to D_s^{\mp} K^{\pm}) = [2.4^{+1.2}_{-1.0}(\text{stat.}) \pm 0.3(\text{syst.}) \pm 0.3(f_s)] \times 10^{-3}$ with a significance of 3.5σ [4]. The ratio $\mathscr{B}(B_s^0 \to D_s^{\mp} K^{\pm})/\mathscr{B}(B_s^0 \to D_s^- \pi^+) = (6.5^{+3.5}_{-2.9})\%$ is consistent with CDF result $(9.7 \pm 2.0)\%$ [5]. Belle also measured the B_s^* and B_s mass: $m_{B_s^*} = (5416.4 \pm 0.4 \pm 0.5)$ MeV$/c^2, m_{B_s} = (5364.4 \pm 1.3 \pm 0.7)$ MeV$/c^2$ [4].

1.2 First measurement of $B_s \to X^+ l^- \nu$

The total inclusive decay $B_s \to X^+ l^- \nu$ is interesting because its branching fraction can be compared to the total semileptonic B^0, B^+ branching fractions, where significant difference would indicate an unknown source of lepton production in B decays.

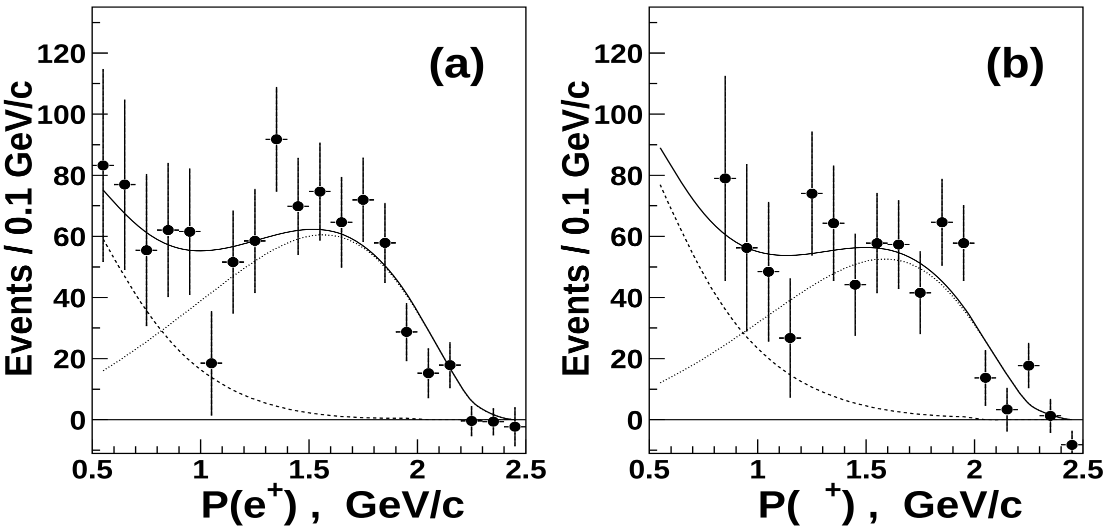

Figure 4: The electron (a) and muon (b) momentum distributions from B_s. They are fitted with primary (dotted) and secondary (dashed) lepton spectra.

Belle reconstructed the same-sign D_s^+ meson and lepton events and obtained the distribution of the lepton momentum, by fitting the D_s^+ mass spectra in each lepton momentum bin. The same-sign requirement suppresses continuum and $B\bar{B}$ backgrounds. Then, the background due to $\Upsilon(5S) \to B\bar{B}(X)$ decay is evaluated using the momentum-corrected $\Upsilon(4S) \to B\bar{B}$ data. The background due to continuum is evaluated using the continuum data. Other mis-ID backgrounds are evaluated using MC. After subtracting the backgrounds above, the lepton momentum distribution is further corrected for the radiative energy loss. Finally, it is efficiency-corrected and plotted in Fig. 4. It is then fitted with two components: primary lepton and secondary lepton spectrum from B_s. The normalizations are floated and shapes fixed from MC. But fitting the electron and muon distributions separately and simultaneously, Belle obtained $\mathscr{B}(B_s^0 \to X^+e^-\nu) = (10.9 \pm 1.0 \pm 0.9)\%$, $\mathscr{B}(B_s^0 \to X^+\mu^-\nu) = (9.2 \pm 1.0 \pm 0.8)\%$, and $\mathscr{B}(B_s^0 \to X^+l^-\nu) = (10.2 \pm 0.8 \pm 0.9)\%$, which is consistent with the PDG value for B^0: $\mathscr{B}(B^0 \to X^+l^-\nu) = (10.33 \pm 2.8)\%$.

1.3 Measurement of $B_s \to J/\psi\phi$ and observation of $B_s \to J/\psi\eta$

B_s decaying to CP eigenstate $J/\psi\phi$ and pure CP eigenstate $J/\psi\eta$ are studied at Belle. J/ψ is reconstructed in the e^+e^- and $\mu^+\mu^-$ channels and the ϕ and η mesons are reconstructed in $\phi \to K^+K^-$ and $\eta \to \gamma\gamma, \pi^+\pi^-\pi^0$ channels, respectively.

The scatter plots for $J/\psi\phi$ are shown in Fig. 5, from which we count the events in signal region and obtain the branching fractions $\mathscr{B}(B_s \to J/\psi\phi) = (1.15^{+0.28}_{-0.30}) \times 10^{-3}$.

The 2D distribution $\Delta E, M_{\rm bc}$ for $J/\psi\eta$ are fitted for the two η channels, and projected in Fig. 6. The background shapes are all flat and the normalization for $J/\psi X$ background is fixed. We obtain $\mathscr{B}(B_s \to J/\psi\eta) = (3.44 \pm 1.07(\text{stat.})^{+0.62}_{-0.30}(\text{syst.})) \times 10^{-4}$ in $\eta \to \gamma\gamma$ channel, and $\mathscr{B}(B_s \to J/\psi\eta) = (4.60 \pm 2.06(\text{stat.})^{+0.89}_{-0.30}(\text{syst.})) \times 10^{-4}$ in $\eta \to \pi^+\pi^-\pi^0$ channel, combined to $\mathscr{B}(B_s \to J/\psi\eta) = (3.69 \pm 0.95(\text{stat.})^{+0.65}_{-0.30}(\text{syst.})) \times 10^{-4}$.

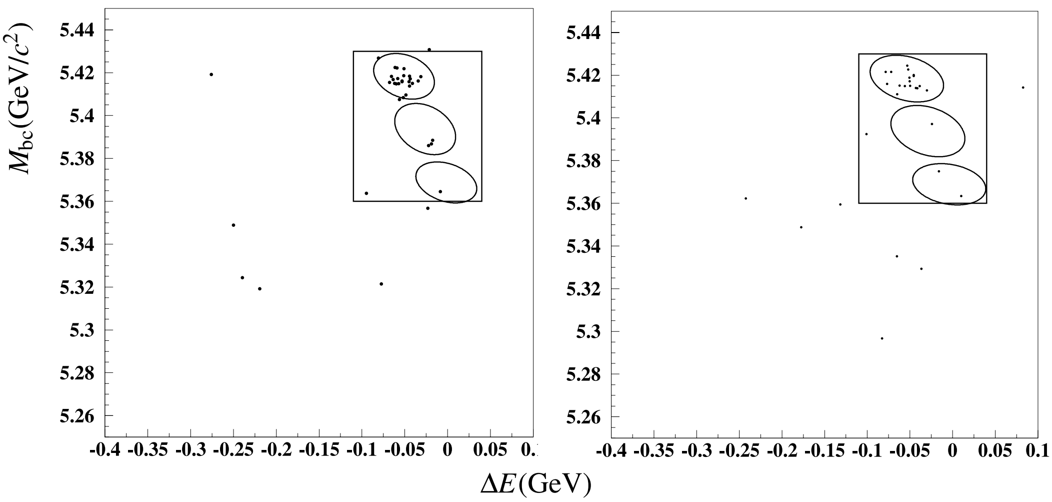

Figure 5: $M_{\rm bc}$ v.s. ΔE scatter plots for $B_s \to J/\psi\phi$. The left corresponds to $J/\psi \to \mu^+\mu^-$ and the right corresponds to $J/\psi \to e^+e^-$.

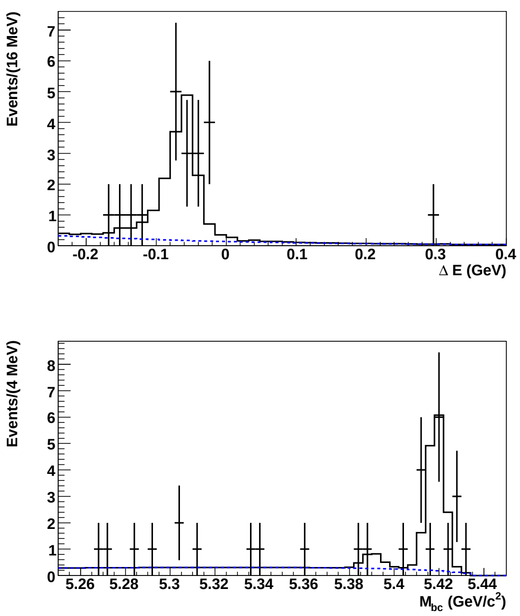

Figure 6: Data projection from the $B_s^* B_s^*$ signal region onto the ΔE and $M_{\rm bc}$ axis for the combined $J/\psi\eta$ channels. Background is represented with the dashed curve.

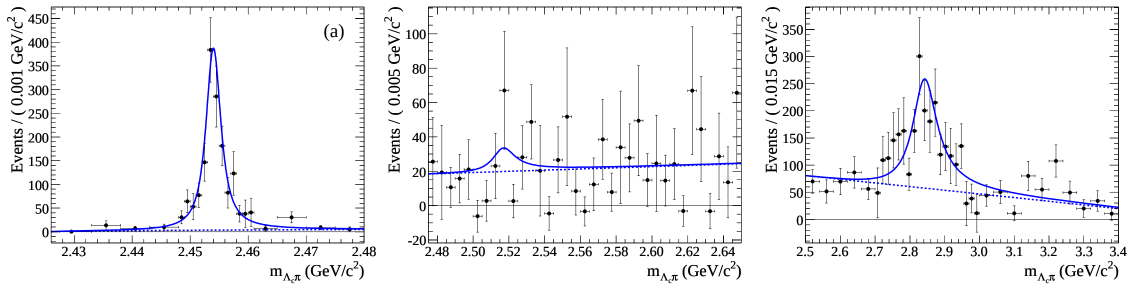

Figure 7: Background free projections of $m_{\Lambda_c\pi}$ in regions of $\Sigma_c(2455)^0$, $\Sigma_c(2520)^0$ and $\Sigma_c(2800)^0$ mass.

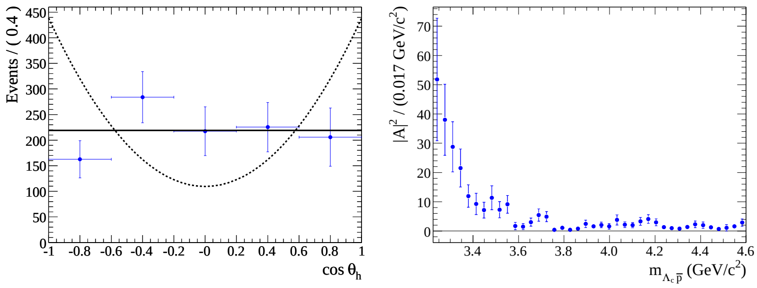

Figure 8: Distributions for helicity angle for $\Sigma_c(2455)^0$ candidates (left), and the invariant mass $m_{\Lambda_c\bar{p}}$ (right). The solid line is for spin-1/2 and the dashed line is for spin-3/2 hypothesis.

2. Charmed Baryonic B decay

Study of baryonic B decay provides a laboratory to study baryon production mechanisms, search for exotic states and to determine baryon spins.

BaBar studied the B decays to $\Lambda_c^+\bar{p}(\pi^-)$ and measured the ratio of branching fractions $\mathscr{B}(B^-\to\Lambda_c^+\bar{p}\pi^-)/\mathscr{B}(\overline{B}^0\to\Lambda_c^+\bar{p}) = 15.4\pm1.8\pm0.3$ [7], which is qualitatively consistent with the theoretical argument that B decays are favored if the baryon and antibaryon are close in phase space. In the two-body case, the baryon-antibaryon has to be back-to-back which cannot be close in phase space.

By studying the mass spectrum of $\Lambda_c^+\bar{p}$ in $B^-\to\Lambda_c^+\bar{p}\pi^-$ decay, BaBar found a significant $\Sigma_c(2455)^0$ signal, no significant signal for $\Sigma_c(2520)^0$, and observed a state assumed to be $\Sigma_c(2800)^0$, as shown in Fig. 7. By studying the helicity angle of the Λ_c^+ or $\bar{p}$ in the $\Sigma_c(2455)^0$ signal region, as shown in Fig. 8, the $\Sigma_c(2455)^0$ is consistent with spin $J=1/2$ and the hypothesis $J=3/2$ is excluded at $>4\sigma$ level. Also, by looking at the mass distribution of $\Lambda_c\bar{p}$ system, a threshold enhancement is seen in the low baryon antibaryon mass distribution shown in Fig. 8. This enhancement is consistent with what is observed in other baryonic modes such as $B\to p\bar{p}K$.

Belle recently studied the decay $\overline{B}^0\to\Sigma_c(2455)^0\bar{p}\pi^+$ by selecting $\Sigma_c(2455)^0\to\Lambda_c^+\pi^-$ candidates from the $\Lambda_c^+\bar{p}\pi^+\pi^-$ final state. This decay has been previously studied by Belle [8] . By fitting the $M(\bar{p}\pi^+)$, $\cos\theta_p$ distribution, Belle finds an enhancement near the mass $M(\bar{p}\pi^+)=1.5$ GeV. We parameterize this excess as a P-wave resonance N^0, and find a a yield of 70 ± 11 with significance 6.1σ. We measure its mass $M=1516\pm29\pm14$ MeV/c^2 and width $\Gamma=365\pm97\pm90$

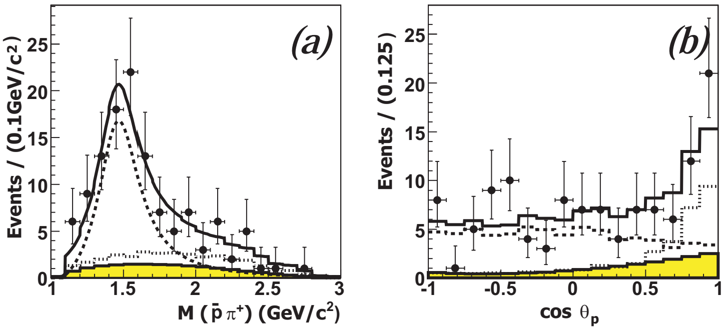

Figure 9: Fit to the $M(\bar{p}\pi^+)$ and $\cos\theta_p$ distributions. The curves represent components of $\bar{B}^0 \to \Sigma_c^0 \bar{N}^0$ (dashed), $\bar{B}^0 \to (\Sigma_c^0\pi^+)_X\bar{p}$ (dotted), the background (shaded) and the sum (solid).

MeV. In the fit, an additional $X^+_{\Sigma_c^0\pi^+}$ resonant component is added to account for the peaking in the $\bar{p}$ helicity angle $\cos\theta_p$ in $\bar{p}\pi^+$ rest frame, as shown in Fig. 9. The branching fraction product is measured to be $\mathscr{B}(\overline{B}^0 \to \Sigma_c(2455)^0\bar{N}^0) \times \mathscr{B}(\bar{N}^0 \to \bar{p}\pi^+) = (0.80 \pm 0.15(\text{stat.}) \pm 0.14(\text{stat.}) \pm 0.21) \times 10^{-4}$, where the last error is due to the uncertainty in $\mathscr{B}(\Lambda_c^+ \to pK^-\pi^+)$.

3. Doubly charmed B decay $(b \to c\bar{c}s)$ and singly charmed B decay with $s\bar{s}$ popping

Belle has also recently investigated B decays to D_s or excited $c\bar{s}$ final states using 657M $B\bar{B}$ pairs. Belle studied the double charmed decay $B \to D_{s1}(2536)^+D^{(*)}$ where D_{s1} is a narrow P-wave ($J^P = 1^+$) $c\bar{s}$ resonance. By fitting $D_{s1}(2536)$ mass simultaneously to three D_{s1} decay channels $[D^{*0}(D^0\gamma)K^+, D^{*0}(D^0\pi^0)K^+, D^{*+}(D^0\pi^+)K_S]$ with no peaking background as studied from ΔE,M_{bc},D^0,D^* sidebands, the branching fractions are obtained as $\mathscr{B}(B^+ \to D_{s1}^+\overline{D}^0) = (3.99 \pm 0.84 \pm 0.57) \times 10^{-4}$, $\mathscr{B}(B^+ \to D_{s1}^+D^-) = (2.76 \pm 0.63 \pm 0.35) \times 10^{-4}$, $\mathscr{B}(B^+ \to D_{s1}^+D^{*-}) = (5.03 \pm 1.21 \pm 0.68) \times 10^{-4}$. Here D_{s1} is assumed to decay solely to two modes $(D^{*0}K^+, D^{*+}K^0)$. The results are consistent with BaBar's result [10].

The decay $B^+ \to D_s^{(*)-}X$ with opposite-sign B and $D_s^{(*)}$ can only proceed with $\geq$ 3body decay and requires a $s\bar{s}$ pair popping besides the $b \to c\bar{u}d$ process. By studying $B^+ \to D_s^{(*)-}K^+\pi^+$ decay, one can study this production mechanism, as well as any charm resonance from $D_s^{(*)-}K^+$ pair since $D_s^{(*)-}\pi^+$ and $K^+\pi^+$ cannot be from normal $q\bar{q}$ resonance.

Belle performed a 3D fit to $(M_{\text{bc}}, \Delta E, m(D_s^{(*)}))$. Projections of these fits onto the M_{bc} axis are shown in Fig. 10 from which we obtain the branching fractions [11] $\mathscr{B}(B^+ \to D_s^-K^+\pi^+) = (1.94^{+0.09}_{-0.08}(\text{stat.})^{+0.20}_{-0.20}(\text{syst.}) \pm 0.17(\mathscr{B}_{\text{int}})) \times 10^{-4}$, $\mathscr{B}(B^+ \to D_s^{*-}K^+\pi^+) = (1.47^{+0.15}_{-0.14}(\text{stat.})^{+0.19}_{-0.19}(\text{syst.}) \pm 0.13(\mathscr{B}_{\text{int}})) \times 10^{-4}$, where $\mathscr{B}_{\text{int}}$ denotes the systematic error due to intermediate sub-branching ratios. These are consistent with BaBar's results [12]. Enhancements in the low mass region of $m(D_s^{(*)-})K^+$ are seen in both modes, as shown in Fig. 11. The enhancements, also seen by BaBar (Fig. 12), may due to a $D_s^{(*)-}K$ resonance. In addition, BaBar also studied more $D_s^{(*)-}hh$ modes, and obtained branching fractions $\mathscr{B}(B^0 \to D_s^-K_S^0\pi^+) = (0.55 \pm 0.13 \pm 0.10) \times 10^{-4}$, $\mathscr{B}(B^0 \to D_s^{*-}K_S^0\pi^+) = (0.29 \pm 0.18 \pm 0.07) \times 10^{-4}$, $\mathscr{B}(B^0 \to D_s^-K^+K^+) = (0.11 \pm 0.04 \pm 0.02) \times 10^{-4}$, $\mathscr{B}(B^0 \to D_s^{*-}K^+K^+) = (0.07 \pm 0.06 \pm 0.02) \times 10^{-4}$.

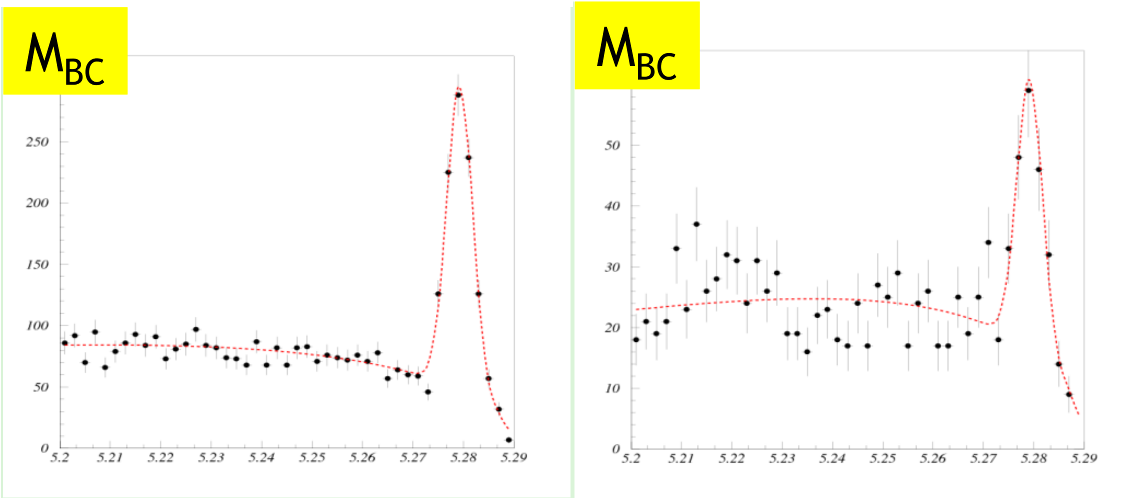

Figure 10: Projections of $M_{\rm bc}$ in the $(\Delta E, M(D_s^{*-}))$'s signal region for $B^+ \to D_s^- K^+ \pi^+$ (left) and $B^+ \to D_s^{*-} K^+ \pi^+$ (right) decays, with all sub modes added.

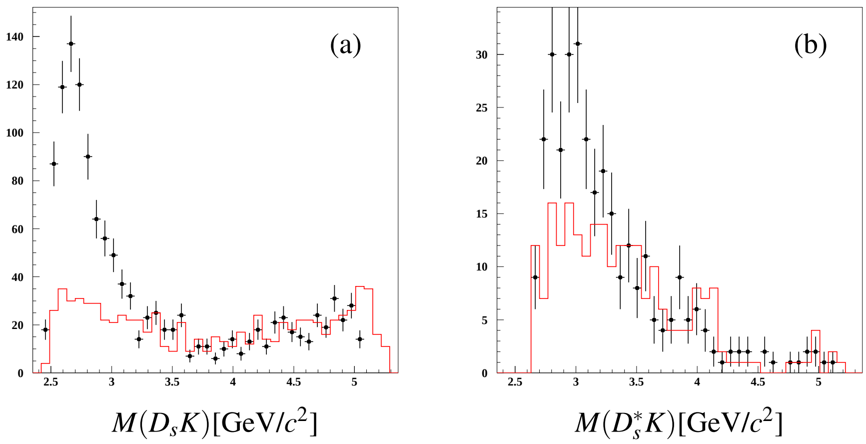

Figure 11: The invariant mass distributions for (a) $D_s^- K^+$ and (b) $D_s^{*-} K^+$ for $B^+ \to D_s^{(*)-} K^+ \pi^+$ decay in the signal regions. The histograms show the background contributions from ΔE sideband.

4. Summary

In summary, recent results in B_s decay and charmed B meson decay are reported. BaBar studied the decay $\overline{B}^0 (B^-) \to \Lambda_c^+ \bar{p} (\pi^-)$, and observed a resonance $\Sigma_c(2800)^0$ and a threshold enhancement in $\Lambda_c \bar{p}$ system. Belle studied the decay $\overline{B}^0 \to \Sigma_c(2455)^0 \bar{p} \pi^+$ and observed an enhancement in the $\bar{p}\pi^+$ invariant mass, which is consistent with a baryonic resonance. Belle and BaBar measured the branching fractions for doubly charmed decay $B \to D_{s1}(2536)^+ D^{(*)}$ and $s\bar{s}$ popping processes $B^{+/0} \to D_s^{(*)-} hh$, which are consistent with each other. Belle measured the absolute branching fractions for $B_s \to D_s^- h$ and the inclusive B_s semileptonic decay, the B_s^* mass, and observed a CP

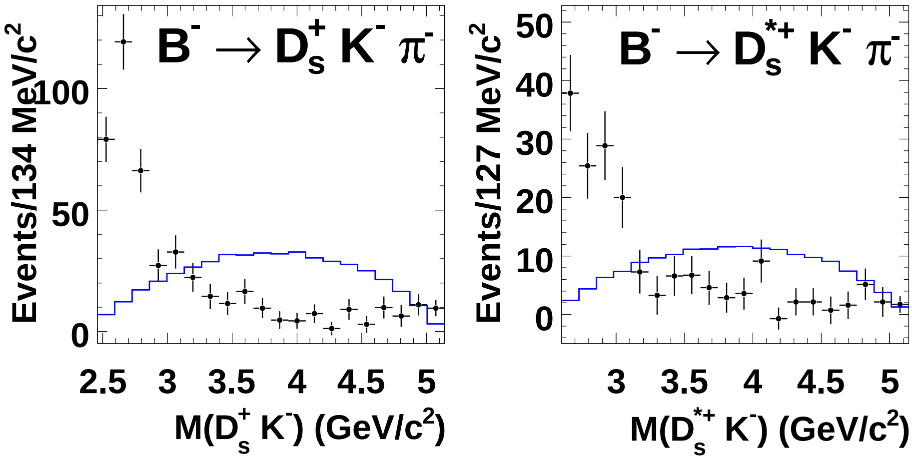

Figure 12: $D_s^{(*)+}K^-$ invariant mass spectra for the $B^- \to D_s^+ K^- \pi^-$ (left) and $B^- \to D_s^{*+} K^- \pi^-$ (right) decay modes using the data. The histograms show the phase space distributions.

eigenstate decay $B_s \to J/\psi\eta$. More B_s results will come with $\sim 100\text{fb}^{-1}$ $\Upsilon(5S)$ data from Belle before the end of year 2009.

References

[1] A. Drutskoy *et al.* [Belle Collaboration], Phys. Rev. Lett. **98**, 052001 (2007) [arXiv:hep-ex/0608015].

[2] G. S. Huang *et al.* [CLEO Collaboration], Phys. Rev. D **75**, 012002 (2007) [arXiv:hep-ex/0610035].

[3] Yu. A. Simonov and A. I. Veselov, JETP Lett. **88**, 5 (2008) [arXiv:0805.4518 [hep-ph]].

[4] R. Louvot *et al.* [Belle Collaboration], Phys. Rev. Lett. **102**, 021801 (2009) [arXiv:0809.2526 [hep-ex]].

[5] T. Aaltonen *et al.* [CDF Collaboration], arXiv:0809.0080 [hep-ex].

[6] K. Abe *et al.* [Belle Collaboration], arXiv:0710.2548 [hep-ex].

[7] B. Aubert *et al.* [BABAR Collaboration], Phys. Rev. D **78**, 112003 (2008) [arXiv:0807.4974 [hep-ex]].

[8] K. S. Park *et al.* [Belle Collaboration], Phys. Rev. D **75**, 011101 (2007) [arXiv:hep-ex/0608025].

[9] H. O. Kim *et al.* [Belle collaboration], Phys. Lett. B **669**, 287 (2008) [arXiv:0808.3650 [hep-ex]].

[10] B. Aubert *et al.* [BABAR Collaboration], Phys. Rev. D **77**, 011102 (2008) [arXiv:0708.1565 [hep-ex]].

[11] J. Wiechczynski *et al.* [Belle Collaboration], arXiv:0903.4956 [hep-ex].

[12] B. Aubert *et al.* [BABAR Collaboration], Phys. Rev. Lett. **100**, 171803 (2008) [arXiv:0707.1043 [hep-ex]].